

# Brazing of reaction-bonded silicon carbide and Inconel 600 with an iron-based alloy

J. R. MCDERMID, R. A. L. DREW

*Department of Mining and Metallurgical Engineering, McGill University, Montreal, Canada*

The objective of the present work was to join reaction-bonded silicon carbide to Inconel 600 (IN600, a nickel-based superalloy) for use in high temperature applications by brazing with an Fe-20 wt% alloy. This joining method resulted in the molten filler metal reacting with the IN600 to form a Ni-Fe-Si solution, which in turn formed a liquid with the free silicon phase of the RBSC. This liquid reacted vigorously with the SiC component of the RBSC to form low melting point phases in both starting materials and chromium carbides at the metal-ceramic interface. By using solution thermodynamics, it was shown that a Ni-Fe-Si liquid with equimolar nickel and iron contents and silicon content of less than 30 at% Si will decompose  $\alpha$ -SiC at the experimental brazing temperatures; it was also shown that these predictions agree with the experimentally observed microstructures and line composition profiles.

## 1. Introduction

The non-oxide silicon-based ceramics (i.e.  $\text{Si}_3\text{N}_4$  and SiC family of ceramics) have outstanding high temperature strength and creep resistance as well as low coefficients of thermal expansion (CTE) and, therefore, good thermal shock resistance [1]. Large or complex ceramic parts are difficult and expensive to manufacture, thus ceramic parts tend to be of simple shape and small in size. In order for these ceramics to be assembled into more complex parts and to maximize their performance in advanced heat engines, it is necessary to successfully interface them with other ceramics and the existing metallic support structure. In advanced heat engines, particularly gas turbines, this would entail the joining of ceramics to nickel, cobalt or iron-based superalloys such that the joints could withstand the high temperatures ( $> 1000^\circ\text{C}$ ) and aggressive oxidizing environment of the engine. In the present work, the joining of reaction-bonded silicon carbide (RBSC) to Inconel 600 (IN600, a nickel-based superalloy) for use in high temperature applications will be considered.

Chemical incompatibility between the metal and ceramic can result in the formation of undesirable phases due to reactions occurring during the joining process. In the case of  $\text{Si}_3\text{N}_4$  and SiC ceramics interfaced with nickel-based superalloys, it has been shown by Mehan and co-workers [2-4] and Jackson and Mehan [5] that extensive chemical reactions will occur if these materials are held in intimate contact at elevated temperatures for extended periods of time, resulting in the formation of metal silicide and carbide phases. In particular, the reaction between RBSC and nickel-based superalloys was found to be quite vigorous [4, 5]. Previous work by the authors [6] has shown that RBSC reacts quickly and vigorously with liquid nickel-based brazing alloys, resulting in the formation of

nickel silicides and chromium carbides through the decomposition of the SiC component of the RBSC. In both cases, it was concluded that the severity of the reaction was greatly enhanced by the nickel alloy forming a Ni-Si liquid with the silicon continuous phase of the RBSC [4-6].

CTE mismatch stresses between the metal and ceramic, resulting from the cooling of the joint from the bonding temperature, tend to manifest themselves as high stress gradients in the region of the metal-ceramic interface [7-9]. CTE mismatch stresses usually result in a reduction of the joint strength or in failure of the joint at the metal-ceramic interface.

High temperature brazing is one of the joining techniques currently enjoying attention for the commercial joining of metals and ceramics. This process requires a wetting liquid at the metal-ceramic interface which forms a continuous layer between the two materials upon solidification. To ensure reproducible mechanical properties of the joint, the filler material layer should be free of voids and other stress concentrators. Also, although some reaction between the filler material and base materials is essential for joining to occur, the brazing process should not significantly affect the properties of the base materials [10]. In brazing, generally, wetting of the ceramic by the liquid filler material and CTE mismatch stresses are the most difficult problems to overcome. If insufficient wetting of the ceramic is achieved by using only the liquid metal on the ceramic surface, then the ceramic surface may be altered by metallizing or by making the brazing alloy active through alloying additions of Ti [10-12]. The latter method, using Ag-Cu alloys with 1.5 to 5 wt% Ti additions, is currently being used to successfully join  $\text{Si}_3\text{N}_4$  and metals [13-17]. These alloys also have the additional advantage of being fairly ductile and are, therefore, able to take up much

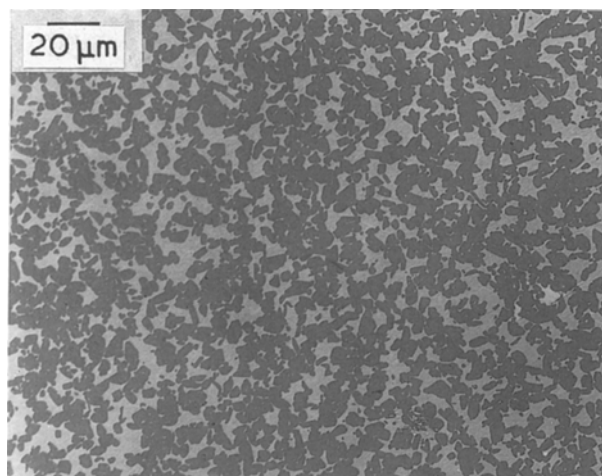


Figure 1 Optical micrograph of as-received RBSC.

of the CTE mismatch stresses through plastic deformation. The melting points of these alloys are usually in the range of 600°C, thus they are not suitable for high-temperature applications [10, 11, 13–17].

The objective of the present study was to join reaction-bonded silicon carbide (RBSC) to Inconel 600 (IN600) using an iron-based brazing alloy. Reasons for using this particular joining system will be outlined below.

## 2. Experimental procedure

Experimental materials consisted of reaction-bonded silicon carbide (RBSC) and hot rolled Inconel 600 (IN600) bar. The iron–silicon brazing alloys used throughout the brazing experiments were manufactured in-house by intimately mixing high purity iron and silicon powders of less than 15 μm equivalent spherical diameter.

The RBSC consisted of SiC grains contained within a continuous silicon phase; the details of the manufacture of this material are given elsewhere [18]. The composition of the RBSC was determined using X-ray powder diffraction (XRD) and the internal standard technique [19], 10 wt % NaCl being the internal standard. It was found that the RBSC consisted of α-SiC and cubic silicon, the silicon phase comprising 13.4 at % of the starting material. This finding was later confirmed using image analysis on a number of representative micrographs, one of which can be seen in Fig. 1. In this case, the light phase is the silicon and the dark phase is the α-SiC grains.

The IN600 and brazing alloys were chemically analysed using atomic absorption spectroscopy. A summary of the compositions of all starting materials can be seen in Table I. This particular series of filler material compositions was chosen because the lowest

TABLE I Starting material compositions (at %)

Material	Ni	Cr	Si	Fe	α-SiC
RBSC	NA	NA	13.4	NA	86.6
IN600	Balance	16.4	NA	6.7	NA
FS1	NA	NA	26	74	NA
FS2	NA	NA	34	66	NA
FS3	NA	NA	40	60	NA

TABLE II Contact angles of Fe–Si alloys on RBSC

Alloy	Temperature (°C)	Contact angle (deg)
FS1	1300	27.2 ± 3.8
FS2	1250	24.6 ± 4.2
FS3	1350	23.8 ± 3.2

melting temperature eutectic in the Fe–Si system is 1200°C; this would still enable the joint to be functional at 1000°C. Also, it was thought that using an Fe–Si alloy would act as a chemical barrier, preventing the interaction of nickel and the RBSC.

Brazing experiments were performed under one atmosphere of argon in a graphite element resistance furnace contained within a water-cooled steel vessel. Specimens consisted of rectangular blocks (ceramic: 10 × 6 × 3 mm<sup>3</sup>; metal: 10 × 6 × 12 mm<sup>3</sup>) held in a boron nitride (BN) jig to ensure proper alignment of the joint materials throughout the experiment.

Brazing materials were applied in the form of brazing pastes using a small amount of polyethylene glycol (PEG) as a binder. Pastes were applied in quantities sufficient to form a layer 0.5 mm thick upon solidification, as recommended by Nicholas and Mortimer [10] for metal–ceramic brazements. All surfaces were ground to a 15 μm finish and degreased with acetone prior to joining.

The furnace cycle was monitored by a type C thermocouple in conjunction with a chart recorder. A typical brazing cycle consisted of heating at 100°C min<sup>-1</sup> to the appropriate brazing temperature (between 1250 and 1350°C), holding at temperature for between 5 to 20 min and cooling at 20°C min<sup>-1</sup> to ambient temperature.

After removal from the furnace, specimens were examined in cross-section after being polished to a 1 μm finish. Specimens were analysed by optical and scanning electron microscopy (SEM). Analysis of the chemical make-up of the joining systems was done using an energy dispersive spectroscopy (EDS) unit resident on the SEM and by electron probe microanalysis (EPMA). Differential thermal analysis (DTA) was used to determine the melting range of some of the constituents formed during the joining experiments.

## 3. Results and discussion

### 3.1. Wettability experiments

In order to assess the wettability of the various iron–silicon alloys for subsequent joining experiments, sessile drop tests were performed using established procedures [20, 21]. Tests showed that the alloys wet the RBSC surface without the need for prior surface treatment. Values for the contact angles are listed in Table II; it can be seen that all of the contact angles are less than 30°, conforming to the criterion proposed by Moorhead and Keating [22] of a maximum contact angle of 30° to ensure adequate adherence of the filler material to the ceramic. It should be noted that the contact angle decreases as the silicon content of the alloy increases. It is thought that increasing the silicon content makes the liquid alloy more compatible with the RBSC surface.

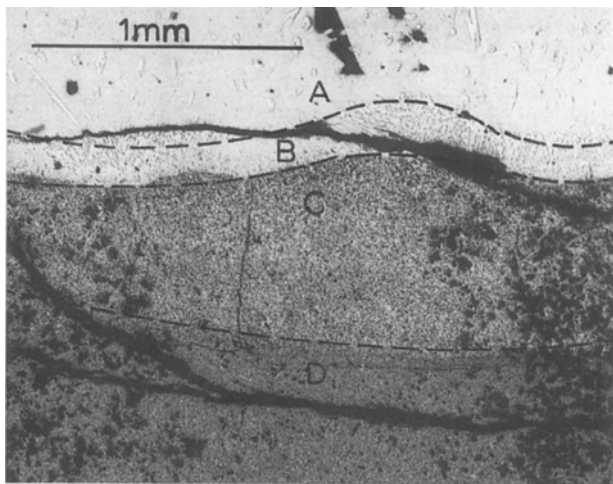


Figure 2 Optical micrograph of IN600–RBSC joint made using FS2 alloy.

Experiments showed, however, that brazing at temperatures exceeding 1250°C caused excessive creep damage to the IN600. In addition, optimum filling of the braze gap was achieved for the FS2 alloy even at this lower brazing temperature. Therefore, this alloy was chosen to be used in all subsequent brazing experiments.

### 3.2. Brazing experiments

An optical micrograph of a brazed joint made using the FS2 alloy and held at 1250°C for 20 min, is presented in Fig. 2. It can be seen from the micrograph that the cross-section can be divided into four distinct zones, annotated A to D in Fig. 2. Transitions between the two zones were based mainly on changes in the microstructure and the EDS profile shown in Fig. 3. Zones in Fig. 3 correspond to those of Fig. 2. The chemical profiles in Fig. 3 were determined by averaging at least three EDS analyses at the appropriate distance from the metal–ceramic interface,

which was originally at the border between zones B and C.

Zone D extends from approximately 1.0 to 3.0 mm from the metal–ceramic interface and was determined, by microanalysis and X-ray mapping, to be characterized by the silicon matrix of the RBSC being transformed into a Si–28Ni–25Fe–5Cr (at %) alloy with the  $\alpha$ -SiC remaining unreacted (see Fig. 4). Compositions shown in Fig. 3 for zone D are for the modified continuous phase only. It must be assumed that this modified continuous phase is the result of the silicon reacting with the iron–silicon brazing alloy; this alloy having previously reacted with the nickel in the IN600 to form a Ni–Fe–Si liquid. This liquid then reacted with the silicon phase of the RBSC, forming more liquid and eventually becoming of fairly homogeneous composition through liquid-phase diffusion. DTA studies showed that the material in both zones C and D had a liquidus of approximately 1025°C. Thus, postulating that the modified silicon phase was formed through liquid phase transport is consistent with this finding.

Zone C extends from the original metal–ceramic interface to approximately 1.0 mm into the RBSC (see Figs 2 and 3). This zone was characterized by the  $\alpha$ -SiC grains of the RBSC being decomposed to form an alloy phase and porosity, as can be seen in Fig. 4. Microanalysis and X-ray mapping showed that the distribution of elements within this zone was homogeneous, further supporting the theory of liquid phase transport of the various elements into the RBSC. Also, the fact that approximately 60 mm<sup>3</sup> of RBSC was decomposed in 30 min (i.e. the total time the joint was above the liquidus of 1000°C) would suggest a liquid–solid reaction since the kinetics are faster than for the corresponding solid state reaction [4, 6].

An examination of Fig. 3 will reveal that nickel and iron are present in nearly equimolar amounts throughout the width of zone C. Using this approximation,

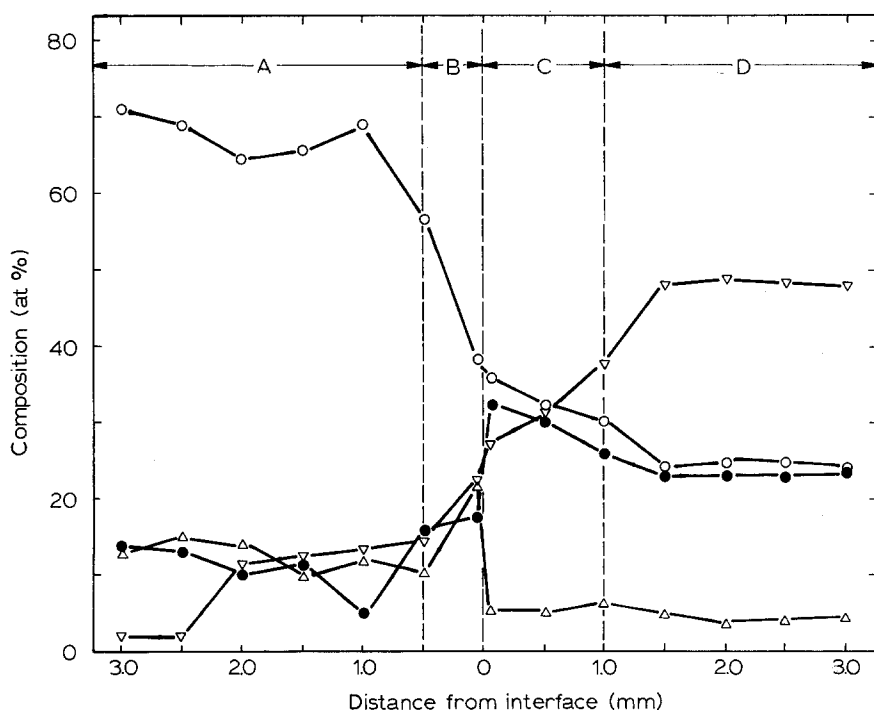


Figure 3 Compositional profile of FS2 brazed joint. (○ nickel, ● iron, ▽ silicon, △ chromium).

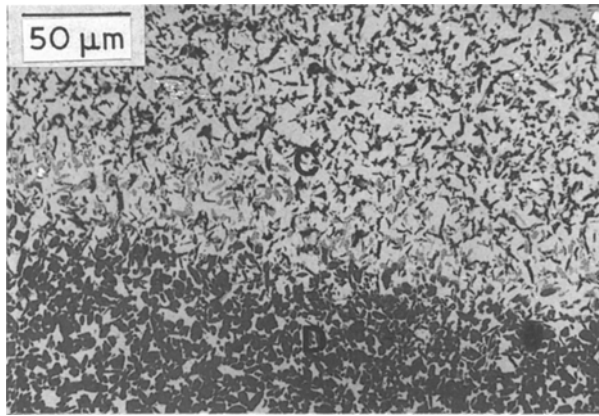
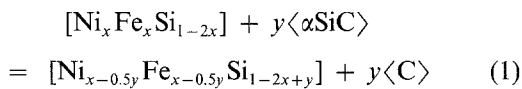


Figure 4 BEI image of zone C-D interface.

the decomposition reaction of the  $\alpha$ -SiC within zone C can be written as



where  $x$  is the atomic fraction of nickel and iron in the Ni-Fe-Si liquid (see Fig. 3) and  $y$  was determined to be 0.05 by calculating the amount of SiC at the reaction interface relative to the amount of Ni-Fe-Si liquid. Square brackets indicate liquid solutions and angular brackets indicate pure solids. Thermodynamic data on the relevant binary systems (Ni-Si, Fe-Si and Ni-Fe) were obtained from Chart [23, 24] and Kubaschewski and Alcock [25]. Data on the pure solids were obtained from Fine and Geiger [26]. The excess molar free energy of the ternary Ni-Fe-Si liquid was then computed assuming regular solution

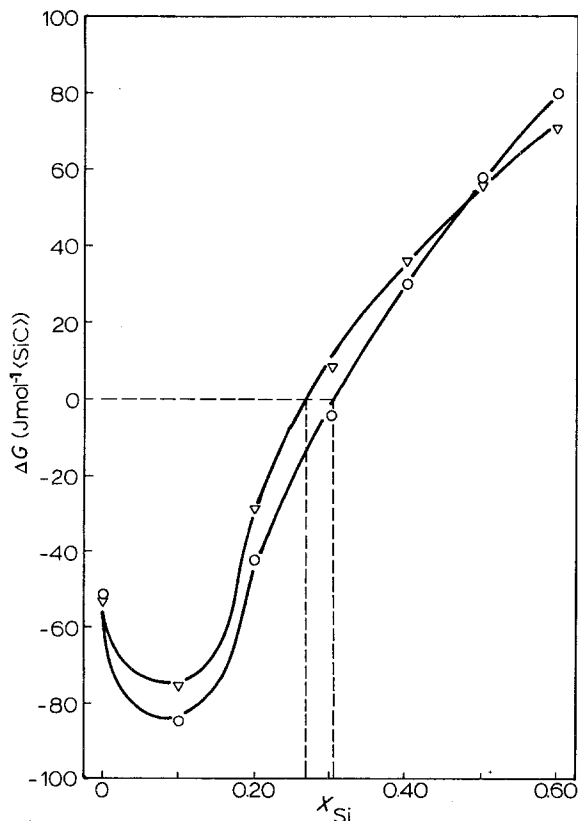


Figure 5  $\Delta G^R$  against atomic fraction (Si) for the  $\alpha$ -SiC decomposition reaction. ( $\nabla$  Kohler,  $\circ$  Toop).

TABLE III Compositions of zones A and B phases

Phase	Location	Composition (at %)
$\gamma$	A and B	$\text{Cr}_7\text{C}_3$ -20Fe (wt %)
$\sigma$	B	Cr-26Ni-18Si-13Fe
$\eta$	A	Ni-15Cr-13Si-5Fe
$\epsilon$	A	Ni-18Si-15Fe-15Cr

behaviour using the Toop [27] and Kohler [28] equations for calculating the excess free energy of ternary solutions from binary solution thermodynamic data.

Using this approximation, a plot of  $\Delta G^R$  for reaction (1) as a function of atomic fraction of Si ( $X_{\text{Si}}$ ) was constructed, the results of which are given in Fig. 5 for both the Toop and Kohler equations. From this figure, it can be seen that the decomposition reaction is favoured for liquids of less than 60 at % Si; which agrees well with the observed microstructure of the joint in zones C and D and with the compositional profiles observed, thus, the modified continuous phase within zone D was not thermodynamically active enough to decompose the SiC within this zone.

XRD analysis of the zone C material determined that it was composed of a mixture of FeSi, FeSi<sub>2</sub>, NiSi and NiSi<sub>2</sub> as well as some phases which were not identified but which were probably complex (Ni, Fe, Cr) silicides. This finding agrees well with published phase diagram data [29].

Zone B is the solidified filler material layer between the RBSC and the IN600 and, thus, is the zone from which the subsequent joining reactions with the RBSC and IN600 originated. A BEI micrograph of zone C is shown in Fig. 6, on which the main phases are shown. EPMA showed that  $\gamma$ -phase as  $\text{Cr}_7\text{C}_3$  with approximately 20 wt % Fe dissolved in it and that the continuous phase ( $\sigma$ ) was Cr-26Ni-18Si-13Fe (at %). The carbon for the formation of  $\gamma$ -phase was supplied by the decomposition reaction of the  $\alpha$ -SiC in the RBSC discussed previously. A summary of the phases found in zone B and their compositions are given in Table III. It was in this zone that the iron-silicon brazing alloy reacted with the IN600 to form a Ni-Fe-Si liquid which subsequently reacted with and decomposed the  $\alpha$ -SiC in the RBSC according to reaction (1).

From the above discussion, the probable sequence of reactions which occurred within the filler material-ceramic system, resulting in the formation of zones B through D, was:

(1) the liquid filler metal reacted with the IN600 to form a Ni-Fe-Cr-Si liquid

(2) this liquid reacted with the silicon in the RBSC, forming a liquid of higher Si content, which entered into the RBSC via the continuous Si phase. This liquid then reacted with the SiC in the RBSC according to reaction (1), the initial value of  $x$  being approximately 0.40 (i.e. 20 at % Si, see Fig. 3). As the reaction proceeded into the RBSC, the amount of silicon in the liquid increased and the value of  $x$  decreased, due to the addition of silicon from the reaction, to the point where reaction (1) was no longer thermodynamically favourable (see Fig. 5). This composition is close to that found at the zone C-D interface.

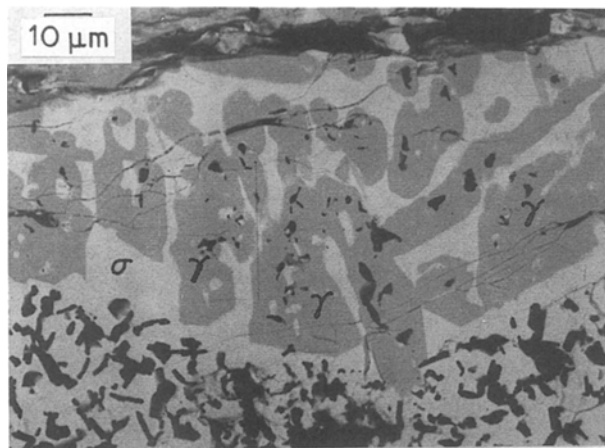


Figure 6 BEI micrograph of zone B.

(3) the liquid continued into zone D by liquid phase diffusion via the Si continuous phase. Due, however, to the higher silicon content of the liquid,  $\Delta G^R$  for reaction (1) was positive and no SiC decomposition occurred within zone D (see Figs 4 and 5).

(4) as the joint cooled to the liquidus temperature of  $1000^\circ\text{C}$ , the carbon, chromium and some of the iron was rejected to the metal–ceramic interface (zone B) to form Cr carbides ( $\gamma$ -phase) and solid solution phases ( $\sigma$ -phase) upon solidification.

A schematic representation of these processes is given in Fig. 7.

Further examination of Figs 2 and 6 will show that there is extensive cracking in zone B along the zone A–B interface (top of the micrograph). This is due mainly to CTE mismatch stresses and is aggravated by the fact that both  $\gamma$  and  $\sigma$  phases are brittle and act as an easy path for the propagation of cracks.

Zone A was formed by the reaction between the IN600 and the liquid iron–silicon filler material. An optical micrograph of Zone A through C is given in Fig. 8. It can be seen that zone A consists of two constituents  $\eta$  and  $\epsilon$ , the compositions of which can be found in Table III. From the compositions of the two phases and by using the relevant phase diagrams [29, 30], it can be inferred that the melting points of the continuous  $\eta$ -phase is approximately  $1100^\circ\text{C}$ , and therefore, the interaction of the liquid iron–silicon filler material with the IN600 has seriously degraded the high temperature properties of the IN600.

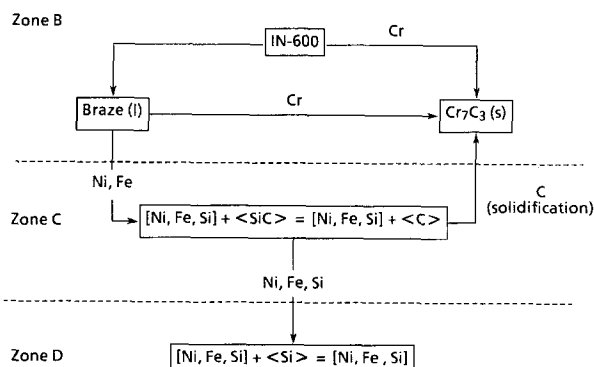


Figure 7 Schematic representation of reactions occurring in zones B to D during the joining process.

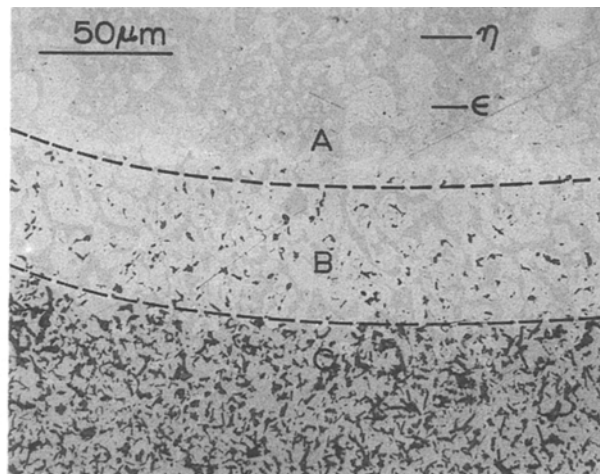


Figure 8 Optical micrograph of zones A to C.

From the above discussion, using an Fe–34Si (at %) alloy to join RBSC to IN600 by direct brazing is not feasible due to the extensive chemical reactions between the filler material and the base materials, resulting in degradation of the high temperature properties of the base materials. In particular, the decomposition of the RBSC by the filler material was especially deleterious. Also, extensive cracking at the metal–ceramic interface occurred because of CTE mismatch, resulting in failure of the joints.

#### 4. Conclusions

The conclusions are as follows.

(1) The presence of a liquid Fe–34Si (at %) filler material in IN600–RBSC joints results in the alloy reacting with both starting materials, forming low-melting point phases and, therefore, degrading the high temperature properties of both starting materials.

(2) Degradation of the RBSC is the result of the liquid filler material combining with the nickel in the IN600 to form a Ni–Fe–Si liquid, which subsequently decomposes the SiC in the RBSC, forming low-melting iron and nickel silicides within the RBSC and chromium carbides at the metal–ceramic interface, the carbon for the carbides being supplied by the SiC decomposition. The carbide was formed at the metal–ceramic interface due to solute partitioning during the solidification of the various constituents.

(3) The large coefficient of thermal expansion mismatch stress generated during cooling and the formation of brittle phases at the metal–ceramic interface resulted in cracking and failure of the joints within this region.

#### Acknowledgements

The authors would like to thank Pratt and Whitney Canada Ltd for sponsoring this work.

#### References

1. D. W. RICHERDSON, in "Modern Ceramic Engineering" (Marcel Dekker, New York, 1982) p. 139.
2. R. L. MEHAN and D. W. MCKEE, *J. Mater. Sci.* **11** (1976) 1009.
3. R. L. MEHAN and R. B. BOLON, *ibid.* **14** (1979) 2471.
4. R. L. MEHAN and M. R. JACKSON, in "Materials

- Science Research", Vol. 14 (Plenum Press, New York, 1981) p. 513.
5. M. R. JACKSON, R. L. MEHAN, A. M. DAVIS and E. L. HALL, *Met. Trans.* **14A** (1981) 355.
  6. J. R. MCDERMID, M. D. PUGH and R. A. L. DREW, *ibid.* **20A** (1989) 1803.
  7. K. SUGANUMA, T. OKAMOTA, M. KOIZUMI and M. SHIMADA, *J. Amer. Ceram. Soc.* **68** (1985) C-334.
  8. K. SUGANUMA, T. OKAMOTA, M. KOIZUMI and K. KAMACHI, *J. Mater. Sci.* **22** (1987) 3561.
  9. J. R. MCDERMID, M. D. PUGH and R. A. L. DREW, in Proceedings of the International Symposium on Advanced Industrial Materials, Montreal, August 1988, edited by D. S. Wilkinson (Pergamon Press, New York, 1989) p. 169.
  10. M. G. NICHOLAS and D. A. MORTIMER, *Mater. Sci. Technol.* **1** (1985) 657.
  11. R. L. TALLMAN, R. M. NEILSON Jr., J. C. MITTL, S. P. HENSLEE and P. V. KELSEY Jr., in Report No. EGG-SCM-6572, Idaho National Engineering Laboratory (1984).
  12. G. R. VAN HOUTEN, *Ceram. Bull.* **38** (1959) 301.
  13. J. A. PASK, *Amer. Ceram. Soc. Bull.* **66** (1987) 1567.
  14. H. MIZUHARA and K. MALLY, *Weld. J.* **64** (1985) 27.
  15. M. MUZHARA, *Adv. Mat. Proc.* **131** (1987) 53.
  16. R. E. LOEHMAN and A. P. TOMSIA, *Ceram. Bull.* **67** (1988) 375.
  17. R. E. LOEHMAN, *ibid.* **68** (1989) 891.
  18. C. W. FOREST, P. KENNEDY and J. V. SHENAN, in "Special Ceramics 5" (British Ceramics Research Association, Stoke-on-Trent, 1972) p. 99.
  19. B. CULLITY, in "Elements of X-ray Diffraction", 2nd Edn (Addison-Wesley, Toronto, 1978) p. 415.
  20. J. A. PASK and R. M. FULRATH, *J. Amer. Ceram. Soc.* **45** (1962) 592.
  21. J. A. PASK and A. P. TOMSIA, in "Materials Science Research", Vol. 14 (Plenum Press, New York, 1981) p. 411.
  22. A. J. MOORHEAD and H. KEATING, in Report No. ORNL-6262, Oak Ridge National Laboratory (1986).
  23. T. G. CHART, National Physical Laboratory Report Chem. 18 (1972).
  24. *Idem*, *High Temp.-High Press.* **2** (1970) 461.
  25. O. KUBASCHEWSKI and C. B. ALCOCK, in "Metallurgical Thermochemistry", 5th Edn (Pergamon Press, Toronto, 1979).
  26. H. A. FINE and G. H. GEIGER, "Handbook on Material and Energy Balances in Metallurgical Processes" (The Metallurgical Society of the AIME, Warrendale, 1979).
  27. G. W. TOOP, *Trans. Met. Soc. AIME* **233** (1965) 850.
  28. F. KOHLER, *Monatsh. Chemie.* **91** (1960) 738.
  29. G. V. RAYNOR and V. G. RIVLIN, *Int. Met. Rev.* **30** (1985) 181.
  30. M. HANSEN, in "Constitution of Binary Alloys", 2nd Edn (McGraw-Hill, New York, 1958).

*Received 26 June  
and accepted 1 December 1989*